Simulation and Analysis of Pull-Up Manoeuvre during In-Air Capturing of a Reusable Launch Vehicle

Sunayna Singh[1*], Leonid Bussler[1], Sven Stappert[1], Martin Sippel[1],
Yakut Cansev Kucukosman[2] and Sophia Buckingham[2]

[1]DLR Institut für Raumfahrtsysteme, Bremen, Germany
**Linzer Strasse 1, 28359, Bremen, Sunayna.Singh@dlr.de*

[2]von Karman Institute for Fluid Dynamics VKI, Belgium
72 Chaussée de Waterloo, Rhode-St-Genèse B-1640, sophia.buckingham@vki.ac.be

Abstract

The innovative 'In-Air-Capturing (IAC)' recovery method involves winged rocket stages being captured mid-air and towed back to the launch site. This patented approach by German Aerospace Center (DLR), shows potential for substantial cost reduction by eliminating the need for an additional propulsion system during descent. A critical operation in IAC involves the Towing Aircraft (TA) and Reusable Launch Vehicle (RLV) performing a coordinated pull-up, such that the configuration transitions from a descending glide to a powered ascending flight. During this maneouvre, the two vehicles are connected to each other by a rope, allowing the TA to use its propulsion system to tow the RLV and gain altitude. The final goal at the end of this maneouvre is to reach a suitable cruise altitude for the tow-back to the launch site. This paper presents the modelling and simulation of a full-scale RLV and TA performing the Pull-Up Maneouvre of IAC. Important subsystems like aerodynamics, propulsion, guidance and control, as well as external disturbances from the wake of the aircraft are discussed in detail. The RLV and TA are assumed to be connected by a simplified rope, modelled as a rigid link. An analysis is performed to determine the optimal cruise flight conditions for the mated configuration. Trajectory simulations are then performed to identify the challenges and additional requirements for the system. From the simulations, it could be concluded that the configuration could reach the commanded cruise conditions despite external disturbances from the wake. To sum up, the potential improvements and future simulations are discussed.

1. Introduction

Over the 21st century, the commercial interest in reusable launch technology has grown tremendously. Reusable Launch Vehicles (RLVs) reduce launch cost through recovery and reuse of parts of the launcher. The currently operational RLVs mostly land vertically using the engines from first stage to slow down. This method requires significant amount of fuel for deceleration and landing, thereby adding to the inert mass and causing a penalty on payload capacity. An innovative approach, called 'In-Air-Capturing (IAC)', which eliminates these disadvantages has been patented by DLR [1]. The idea involves 'the winged stage being caught mid-air and towed back to the launch site without the need of additional propulsion system' [2], [3].

The operational cycle of a mission with IAC starts with the launcher lifting off vertically and ascending until Main Engine Cut-Off (MECO). At MECO, the winged first stage separates from the launch vehicle and re-enters the atmosphere in a ballistic trajectory, in the course of which it decelerates from supersonic velocity to a subsonic glide. Meanwhile, a capturing aircraft is waiting at the downrange rendezvous area, loitering until the RLV arrives. Between 8 km to 2 km altitude, the final IAC manoeuvre is performed [4]. To get a better understanding of the IAC manoeuvre, the process can be divided into five phases as shown in Figure 1:

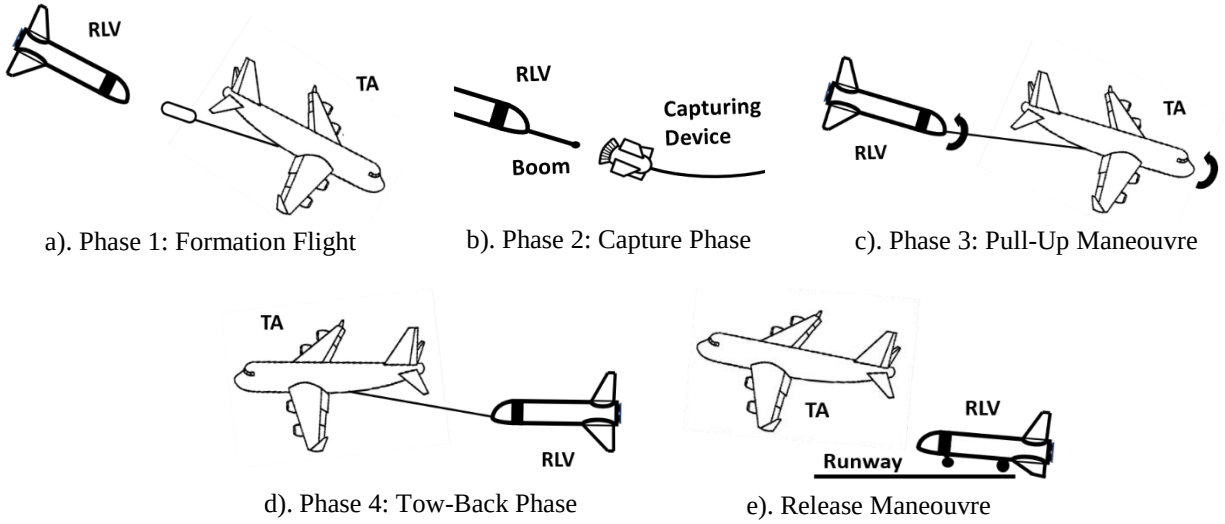

a). Phase 1: Formation Flight b). Phase 2: Capture Phase c). Phase 3: Pull-Up Maneouvre

d). Phase 4: Tow-Back Phase e). Release Maneouvre

Figure 1: Phases of In-Air Capturing Maneouvre

- *Phase 1: Formation Flight*
  During the *formation flight phase* (Figure 1a), the Towing Aircraft (TA) glides from cruise flight and attempts to achieve a parallel descending formation with the RLV. Here, both vehicles attempt to maintain similar velocities and flight path angles, while separated by a safe distance. The formation envelope must be maintained long enough for the *capture phase* to be successfully completed. A detailed analysis of the dynamics and trajectories of this phase can be found in [5].

- *Phase 2: Capture Phase*
  While the two vehicles are in formation, the *capture phase* (Figure 1b) is carried out. A capturing device attached to a rope is first released from the aircraft. This agile device autonomously navigates its way to the RLV and ensures mating of the two vehicles. Once the RLV is connected to the TA via the rope, the aircraft acts like an external propulsion system to the RLV. A detailed modelling of critical aspects like aerodynamics, rope dynamics and control architecture of this phase has been discussed in [6], [7] and [8].

- *Phase 3: Pull-Up Manoeuvre*
  Next the mated configuration in descending flight performs a *pull-up manoeuvre* (Figure 1c) to transition to an ascending flight. During this, the TA engines are turned on to provide thrust to the system. The configuration can then gain altitude and achieve a suitable cruise state.

- *Phase 4: Tow-Back Phase*
  The *tow-back flight* (Figure 1d) simply involves the TA towing the RLV to the landing site. The configuration flies at an optimal altitude and velocity to minimize fuel consumption.

- *Phase 5: Release Manoeuvre*
  The *release manoeuvre* (Figure 1e) involves release of the RLV by the TA close to the runway. The RLV lands horizontally onto the landing strip using its own landing gear.

This paper examines the third phase of IAC, called *pull-up manoeuvre,* using full-scale (or large scale) test cases. The mated diving configuration (connected by a rope) is now required to pull-up to a suitable altitude and achieve cruise flight. For this, the TA exploits its superior aerodynamic performance and powerful propulsion system to tow the RLV to the commanded altitude. The test cases and the important subsystems associated with the simulation of *pull-up maneouvre* are first introduced in Section 2. This includes modelling of the aerodynamics, propulsion and a simplified rope model. Next, the commanded cruise altitude should be selected such that the TA consumes minimum fuel on its trajectory back to the launch site. Based on this, a guidance and control architecture is proposed in Section 3. Lastly, Section 4 analyses the trajectory simulations of *pull-up maneouvre,* followed by the conclusions and future work in Section 5.

2. Modelling of Full-Scale Test Scenarios

The *pull-up maneouvre* starts with the unpowered TA and RLV (linked by a rope) in a rapidly descending flight somewhere between 5000 m and 6000 m altitude [5]. To be able to safely fly back to the launch site, the configuration must now come out of this gliding flight without descending below 3000 m and pull-up to a secure cruise altitude for the *tow-back* phase. Since the RLVs are likely to have lower Lift to Drag (L/D) ratios of between 2-4.5, it cannot pull-up to a higher altitude on its own without any propulsion. Therefore, the TA which tends to have high L/D ratio (up to 20) like most commercial airliners, uses its superior aerodynamics and thrust from its propulsion system to help the RLV reach the commanded altitude. Thus, the success of the maneouvre also depends on the selected full-scale RLV and the TA configurations.

For a realistic simulation of the full-scale scenario of IAC, some important subsystems must be reliably modelled. The trajectory not only depends on the aerodynamics of the vehicles, but also mass configuration, propulsion and external disturbances like wake from the TA. The dynamics from the ropes is also an important factor for this phase. In the coming section, the full-scale test cases are introduced and modelling of these crucial aspects are presented.

2.1 Selected Test Cases

The large-scale test cases that are consistently used in previous studies of IAC ([5], [6], [7] and [8]) are shown in Figure 2 and Figure 3. The RLV is selected to be the first stage of a 3 Stage-To-Orbit (3STO) launch vehicle proposed in [9]. This returning winged stage called RLVC4-IIIB has a special swept wing configuration. The outer wings of the spacecraft are folded in during the hypersonic re-entry to avoid shock-shock interaction. Then, once the vehicle has slowed down to subsonic velocity, the outer wings are deployed (or unfolded) as shown in Figure 2. The larger wings facilitate a higher maximum trimmed L/D ratio of up to 6 in the subsonic regime, making the configuration advantageous for IAC. The configuration uses control flaps for trimming and manoeuvring, which can deflect up to ±20°. The subsonic configuration during descent is expected to weight approximately 80 tons.

Based on the scale of the RLV, a suitably sized TA is selected. For the current application of capturing a large 80-tonne RLV, an Airbus A340-600 (shown in Figure 3) is considered fit [3]. The long-range jetliner with large loading capacity and four powerful Rolls Royce Trent 556 engines can support the towing loads from the large rocket stage. The relatively advanced flight control system is also advantageous for the complex manoeuvres required in IAC. Further, repurposing the retired fleet would not only prove to be economically advantageous but also add a component of reusability to the now withdrawn aircraft. At the start of *pull-up manoeuvre*, the TA is expected to weigh 280 tons [5]. Since no power or thrust was used in the previous phases of IAC (*formation flight* and *capture phase*), the aircraft essentially weighs the same as in the beginning of IAC maneouvre.

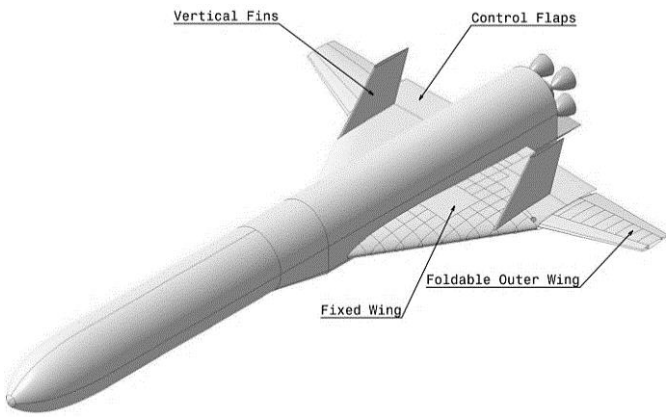

Figure 2: Subsonic Configuration of RLVC4-IIIB [8]

Figure 3: Commercial Airliner: A340-600 [10]

2.2 Aerodynamics

The aerodynamics of the RLV is analysed using Reynolds-Averaged Naviers Stokes (RANS) to achieve high confidence datasets. The CFD simulations are performed using the open source code OpenFOAM v6.0 for a flight point at 6000 m altitude at Mach 0.45. Since the flight point exists in the compressible subsonic flow regime, the rhoSimpleFoam solver is used. The k-ω SST turbulence model is used for accurate representation of the flow. The data was then extended to other Mach numbers using Prandlt-Glauert compressibility corrections [12]. Figure 4 shows the trimmed performance curves achieved for the subsonic RLV configuration. It can be observed that at high angles of attack, the RLV is able to reach a maximum trimmed L/D ratio of slightly higher than 6.

Since the RANS calculations can be computationally very intensive when many datapoints are required, a more simplified approach is used for TA. For the *pull-up maneouvre*, the TA is in its clean configuration trying to achieve its maximum aerodynamic performance. The aerodynamic dataset for TA was again calculated using OpenFOAM, but using the less computationally expensive Euler computations. Since the flow in Euler calculations is considered non-viscous, it is only able to provide good estimates for lift and moment coefficients. The drag coefficient data is therefore estimated using empirical methods. The final database is validated using RANS calculations at a few datapoints based on the available computational resources.

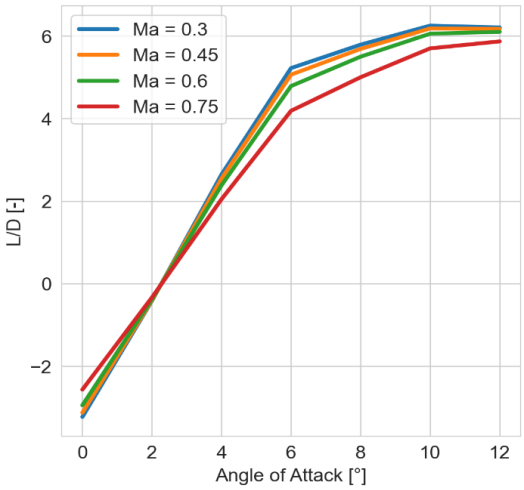

Figure 4: Trimmed Performance Curves of RLV during Pull-Up Maneouvre

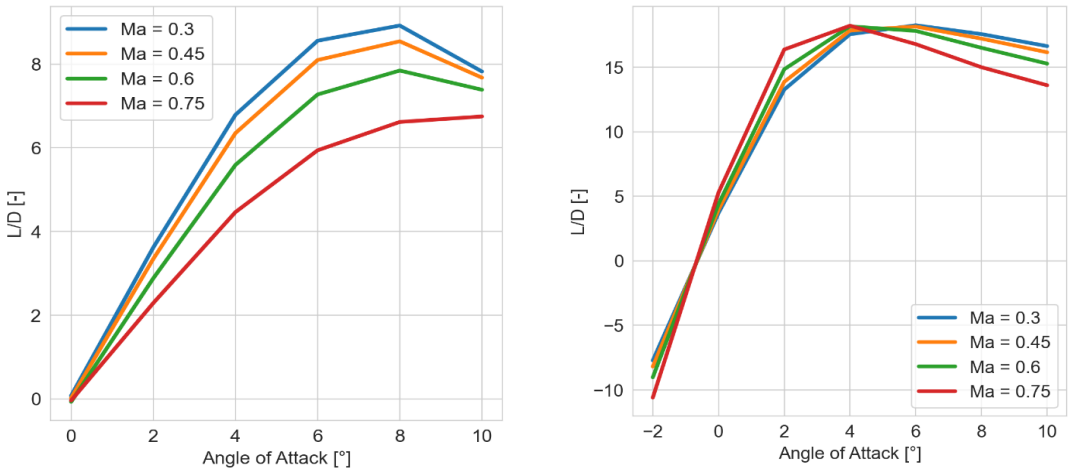

a) TA during Formation Flight

b) TA during Pull-Up Maneouvre

Figure 5: Trimmed Performance Curves for Different TA Configurations in IAC

It must be specified that in the beginning of the *pull-up maneouvre*, the TA configuration undergoes a change. For the previous phases (*formation flight* and *capture phase*), the TA deploys its front and main landing gear as well as the spoilers (-20°). This is done to reduce the gap in aerodynamic performance between TA and RLV, which is essential to maintain the capture window during *formation flight*. A more detailed study can be found in [5]. Once the connection has been established between the two vehicles, the landing gears and spoilers are retracted in preparation for the pull-up. Figure 5 shows the performance of TA configurations before and during the *pull-up maneouvre*. It can be observed that the maximum L/D has a value of 8.5 at 8° angle of attack during *formation flight* (Figure 5a). While during *pull-up maneouvre* (Figure 5a), the maximum L/D of 17.5 is achieved at an angle of attack of 4°. This change in aerodynamic performance of TA is captured in the trajectory simulations through a linear transition between the two datasets performed at the beginning of simulation.

2.3 Propulsion

The propulsion system for TA plays a crucial role in the success of the *pull-up maneouvre*. For the current test scenario, the A340-600 consists of four powerful Rolls Royce Trent 500 engines. These high bypass turbofan engines provide a maximum take-off thrust of 260 kN and a maximum continuous thrust of 197 kN each [12]. Since the performance of an airbreathing engine varies with air density, the engine thrust varies with altitude and Mach number. Such data varies from engine to engine, and is usually not available to public for commercial engines. Thus, to capture the realistic engine performance, an intricate propulsion dataset for Trent 500 is generated using the GasTurb tool [13]. The professional tool provides the possibility to estimate the performance of many standard gas turbine configurations, like a 3-spool turbofan in case of Trent 500. Using generic compressor maps, the gas turbine cycle analysis delivers sufficiently accurate performance data for the intended flight envelope. Figure 6 shows the variation of net thrust per engine and specific fuel consumption with altitude and Mach number assuming the engines are at full-throttle.

2.4 Simplified Rope Model

For the preliminary simulations of the *pull-up maneouvre*, the rope is modelled as massless rigid link. The rope is considered to be attached at the centre of gravity of the TA, while the RLV is assumed to be connected to the rope at its nose. The connection points are modelled as spherical joints that constrain translational motion but not the rotational motion. The schematic of the overall set-up for the *pull-up maneouvre* is shown in Figure 7. In this simplified model, the position of the RLV can be written as a function of TA and the rope angle (since it is rigid). Based on the previous studies performed for *formation flight* [5], the rope is assumed to be 210 m long for the current study. In future, this simplified rigid rope model will be replaced by an elaborate model of the flexible rope, presented in [8].

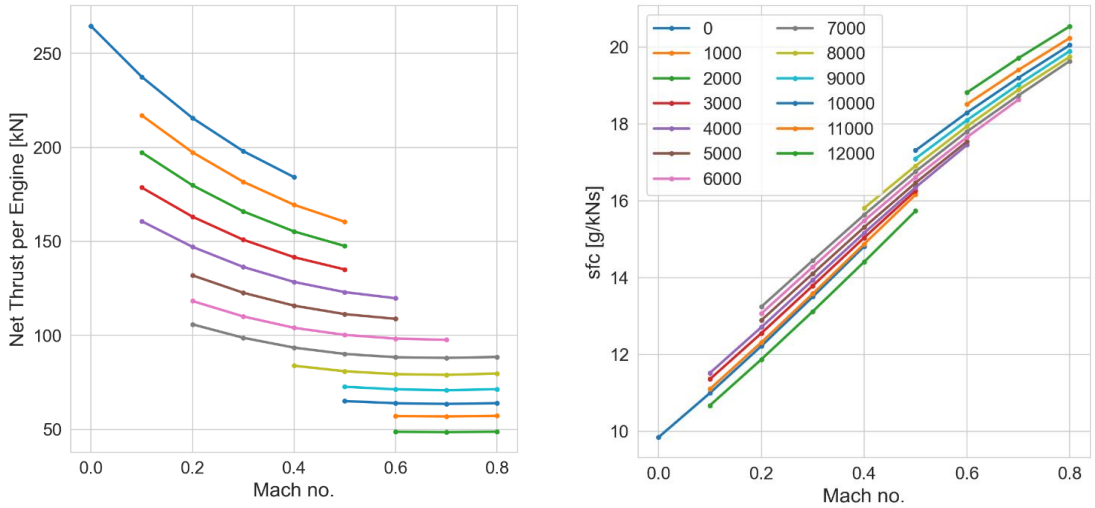

Figure 6: Calculated Performance Maps at Different Altitudes [m] for Rolls Royce Trent-500 at Full Throttle

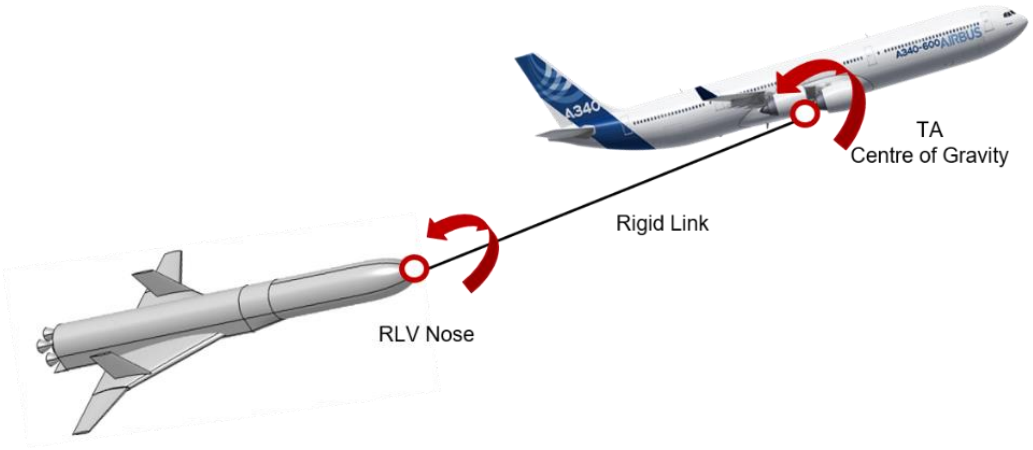

Figure 7: Schematic of Pull-Up Manoeuvre with a Rigid Link connecting the TA and RLV

2.5 Aircraft Wake

During the *pull-up maneouvre*, the RLV remains in close vicinity of the aircraft (150 m for the current test scenario). This means that the aircraft wake can act as a disturbance to the RLV leading to problems during pull-up. During the maneouvre, the aircraft is expected to initially have high angles of attack of up to 12°. Keeping this is mind, RANS calculations were performed to analyse the wake of the A340 at 8° and 12°. Figure 8 shows the velocity contour plots for an angle of attack of 8°. It can be observed that the effect of wake is visible even at a distance of 315 m from the nose of the aircraft.

Figure 8: Wake Velocity Magnitude Contours for Angle of Attack of 8°

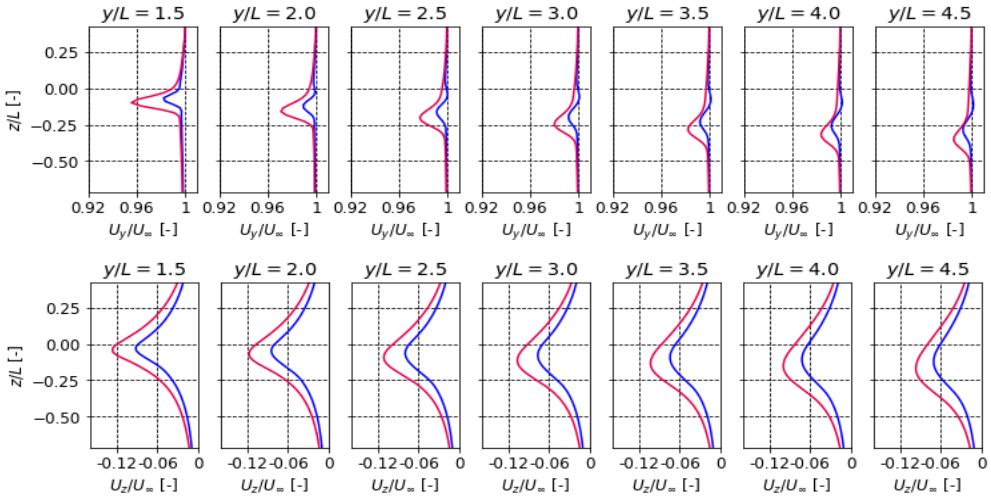

Figure 9: Wake Velocity Components in Fuselage Plane for Aircraft Angle of Attack of 8° (blue) and 12° (red)

Figure 9 provides a closer look on the velocity components of the wake as a function of aircraft length (L) at angles of attack of 8° (blue) and 12° (red). It can be observed from Figure 9 (top) that the horizontal velocity component (U_Y) constitutes a maximum of about 4% of the free stream velocity (U_∞) close to the aircraft. The component gets smaller moving away from the aircraft. However, more concerning magnitudes are observed in the vertical direction (U_Z), which accounts for up to 12% of the free stream velocity (U_∞) at 12° angle of attack. The component does not seem to reduce by a sufficient amount even away from the aircraft. Similar observations can be made for angle of attack of 8°, which accounts for 8% of the free stream velocity in the vertical direction. This vertical deficit in velocity can lead to disturbances in the RLV angle of attack possibly leading to difficulties during the pull-up. Hence, it is critical to analyse the sensitivity of pull-up trajectory to the wake disturbances.

3. Guidance and Control System

The *pull-up maneouvre* would require a coordinated effort to gain altitude by both vehicles. During this phase of IAC, the TA propulsion acts against the drag of the RLV, helping it pull-up to a higher altitude despite its low L/D ratio. At the end of the *pull-up maneouvre*, the configuration should reach a safe altitude and velocity to cruise back to the launch site (*tow-back phase*). Additionally, the target altitude and velocity should be such that minimum fuel is consumed while the RLV is being towed back to the launch site. This optimal cruise condition serves as a guidance command for the *pull-up maneouvre* and is therefore, discussed in further detail in this section. To achieve this, two independent preliminary control algorithms for the TA and RLV are also proposed in this section.

3.1 Optimal Cruise Condition

To determine the optimal cruise conditions at the end of *pull-up maneouvre*, a quasi-optimal approach is used. It is called quasi-optimal because the solution associated with this method is close to optimum, but cannot be considered the optimal solution. It is widely used in traditional engineering applications and well suited for preliminary design (since it does not require definition of complex cost functions fitting all constraints). The idea is to include a preliminary definition of the optimal mode reformulated as a control law, and perform the entire optimization process as a terminal control task [14]. For the cruise condition, the optimal mode for this study is defined as minimum fuel consumption per range. The 3DOF steady flight equations for the complete system (TA and RLV) are first given as follows:

$$m_{TA}\dot{V}_{TA} + m_{RLV}\dot{V}_{RLV} = T + W_{TA}\sin\gamma_{TA} + W_{RLV}\sin\gamma_{RLV} - D_{TA} - D_{RLV} \quad (1)$$

$$m_{TA}V_{TA}\dot{\gamma}_{TA} + m_{RLV}V_{RLV}\dot{\gamma}_{RLV} = L_{TA} + L_{RLV} - W_{TA}\cos\gamma_{TA} - W_{RLV}\cos\gamma_{RLV} \quad (2)$$

Here, the subscripts TA and RLV indicate the properties associated with the respective vehicle. V is the velocity in m/s, m is the mass of the vehicle in kg, L is the lift force in N, D is the drag force in N, T is the thrust from the aircraft in N, W is the weight of the vehicle in N and γ is the flight path angle in radians. Additionally, $\dot{V}$ and $\dot{\gamma}$ indicate the rate of change of velocity in m/s^2 and rad/s respectively.

Further, the forces themselves are calculated as a function of other parameters:

$$D_{TA} = f(H_{TA}, M_{TA}, \alpha_{TA}),\ D_{RLV} = f(H_{RLV}, M_{RLV}, \alpha_{RLV}) \quad (3)$$

$$L_{TA} = f(H_{TA}, M_{TA}, \alpha_{TA}),\ L_{RLV} = f(H_{RLV}, M_{RLV}, \alpha_{RLV}) \quad (4)$$

$$T = f(H_{TA}, M_{TA}, \varepsilon) \quad (5)$$

Here, H is the altitude in m, M is the Mach number, α indicates the angle of attack of the vehicle in radians and ε is the throttle of the engine ranging between 0 and 1. Since the goal is to find a solution for trimmed cruise conditions, some additional simplifications can be made such that:

$$\dot{V}_{TA} = 0, \dot{\gamma}_{TA} = 0, \dot{\alpha}_{TA} = 0, \dot{H}_{TA} = 0 \quad (6)$$

$$\dot{V}_{RLV} = 0, \dot{\gamma}_{RLV} = 0, \dot{\alpha}_{RLV} = 0, \dot{H}_{RLV} = 0 \quad (7)$$

To ensure the stability of the system, an important constraint must be considered. Since the configuration would fly at zero (or near zero) flight path angles during the cruise flight, the RLV must be able to support its own weight by generating sufficient lift. In other words, the vertical steady flight equations for RLV alone during cruise flight must also be included along with Equation (1) and Equation (2). In a simplified form, this can be written as:

$$L_{RLV} = W_{RLV} \cos \gamma_{RLV} \tag{8}$$

Finally, the optimality of the solution is judged using the fuel consumption per range (fcr) for a given flight condition, using the expression:

$$fcr = \frac{sfc.T(H_{TA}, M_{TA}, \varepsilon)}{V_{TA}} \tag{9}$$

Here, sfc is the specific fuel consumption in kg/Ns. Using the above stated equations of motions and the aerodynamic and propulsions datasets shown in the previous sections, stationary solutions can be found. The control parameters such as H, M, α and ε are varied using a grid search and the best of the stationary solutions are sorted using the fuel consumption per range.

Figure 10 shows a number of stationary solutions with different altitude and Mach number combinations, with the fuel consumption indicated by the colour. It was found that many solutions with low fuel consumption per range exist between 6800 m to 8200 m and Mach 0.67 to 0.72. More precisely, it can be observed that the lowest fuel consumption per range is obtained between an altitude of 7800 m and 8200 m, and small velocity range between Mach 0.70 to 0.72. These values were observed for angles of attack close to where TA and RLV reach their maximum L/D value (see Figure 4 and Figure 5). For TA, the angle of attack values for optimal cruise conditions ranged between 3° to 3.5°, while RLV the angle of attack ranged between 6.5° to 8°. Thus, based on these values a commanded altitude of 7800 m at Mach 0.72 is considered as the guidance or target for the terminal state of the *pull-up maneouvre.*

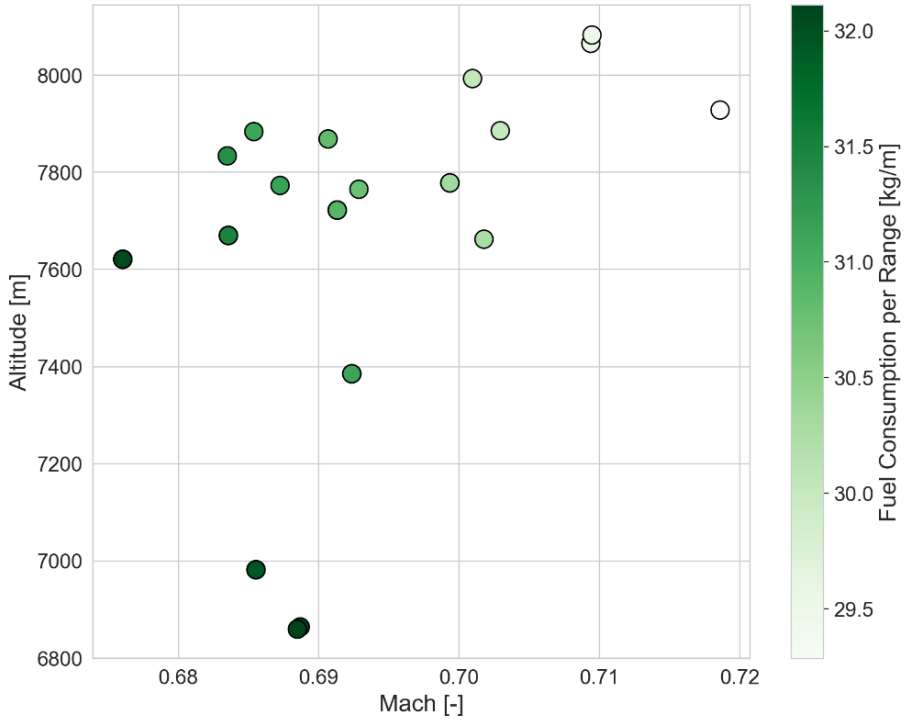

Figure 10: Optimal Cruise Velocity and Altitude based on Fuel Consumption per Range

3.2 Control Architecture

For the pull-up, the mated configuration should have similar positive flight path angle in order to gain altitude. One possible way to achieve this is by commanding the RLV to follow the same flight path angle as that of TA. However, this approach would not be suitable in case of failure or loss of one of the vehicles. There should be a possibility for each vehicle to fly to safety independently in case of emergency. Additionally, flight path angle tracking could also require supplementary sensor fusion and communication links adding to the complexity of the system. Therefore, even though the RLV is connected to the TA via a rope during pull-up, both vehicles are controlled independently. Individual controllers are set up, such that both vehicles are commanded the same target altitude in a coordinate manouvre.

Figure 11 shows the preliminary control architecture for TA (top) and RLV (bottom) used for the *pull-up maneouvre* simulations. The TA consists of an altitude tracking PI controller, for which the control commands are realised through elevators that can deflect between -30° to +15°. It is also possible to control the pitch of the aircraft using the trimmable horizontal stabilizers (that can deflect between -14° to 2°), but they are more suited for trimming and not for rapid maneouvering. Additionally, a PID controller is used to generate throttle commands for the engine (ranging between 10% and 100%) and achieve the commanded velocity. The throttle in turn controls the thrust of the aircraft driving the velocity of both the TA and RLV. The RLV also contains a PI controller to reach the commanded altitude. A PID controller is included for the flight path angle to support the altitude hold during cruise flight. The control commands are realised through flaps that can deflect between ±20°.

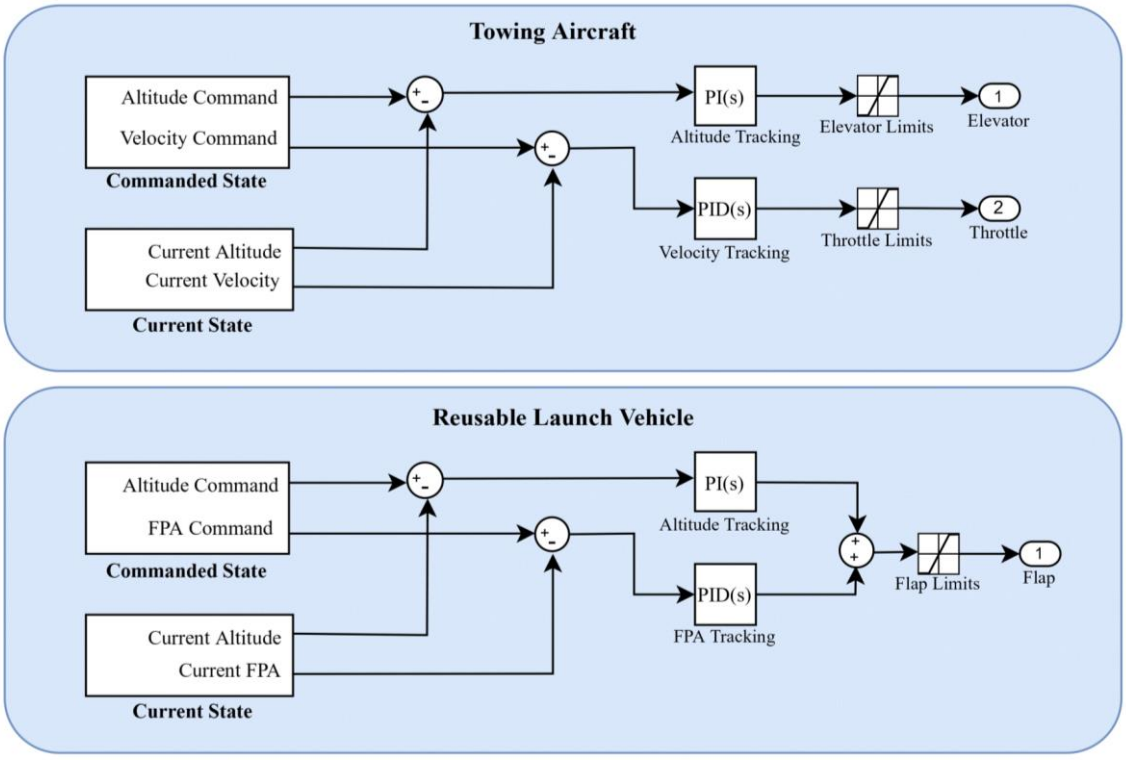

Figure 11: Preliminary Control Architecture for Pull-Up Maneouvre

4. Results

An elaborate model is compiled using all the subsystems stated in Section 2 and Section 3, and linked with environment models like atmosphere, gravity and wind. Assuming a rigid link connecting the RLV to TA, preliminary trajectory simulations are performed and studied in this section.

As mentioned earlier, *formation flight* to *pull-up maneouvre* requires a change of aircraft configuration, which is expected to change the dynamics of the system drastically. Additionally, the previous phases were unpowered, while the current phase requires thrust to pull-up. Therefore, to get a more realistic picture, the trajectory simulation was divided into different steps:

- Step 0 [10 s]: Here, the aircraft retracts its landing gear and spoilers, reducing drag considerably and enabling the aircraft to reach higher L/D ratios (Figure 5). This is represented through a linear transition of aerodynamic datasets from formation flight configuration to pull-up configuration.
- Step 1 [10 s]: Next the aircraft must throttle up from 0% to defined throttle value up to 100%. The turbojet propulsion model is turned on, and can vary between idle thrust (10% throttle) until full-thrust (100% throttle) based on the control input.
- Step 2: This phase constitutes the controlled flight wherein the mated configuration pulls up or climbs from a descending flight to a positive flight path angle based on the target altitude.
- Step 3: Lastly, the altitude hold control or cruise control is performed. This phase continues to the *tow-back phase* until the landing site is reached.

To be able to safely and successfully pull-up, the configuration must come out of the gliding flight before descending below 3000 m altitude. The starting point of simulation is taken as a flight point from the capture margin of the *formation flight* phase shown in [5]. It is assumed that the connection is established at a TA altitude of 5325.5 m and a velocity of approximately 155 m/s. At this point, the configuration is commanded to ascend to an altitude of 7800 m and reach a cruise velocity of 230 m/s (based on the analysis of optimal cruise conditions performed in previous section). The trajectory simulations are first analysed without external disturbances to identify any requirements that are not met by the system. Then, wake is added to the system to analyse the induced disturbances.

4.1 Preliminary Trajectory Simulations

Figure 12 shows the *pull-up maneouvre* trajectory when no aircraft wake is included. The different steps of the simulation are also indicated in the figure. It can be observed that the configuration is able to successfully pull-up to the commanded altitude and velocity within the propulsion capacity of the TA. To quickly transition to an ascending flight, the aircraft angle of attack instantaneously reaches a maximum value of 13°. Such high values of angle of attack (up to 15°) are typically also observed during take-off, and are unlikely to lead to stall. The RLV flight path angle remains quite close to the TA values, leading to a coordinated pull-up effort. Once the cruise altitude is reached, both vehicles maintain a flight path angle of 0° in an attempt to hold the altitude.

Figure 13 shows the control surfaces of the TA (left) and RLV (right) during the *pull-up maneouvre*. It appears that the TA is able to achieve positive flight path with small deflections in elevators, leaving plenty of room for manoeuvrability. The RLV flap on the other hand hits saturation (-20° deflection) during the initial stages of pull-up. The time when the saturation appears, also coincides with the time during pull-up when a larger mismatch in flight path angle was observed between TA and RLV (Figure 12). Although in a simplified simulation with rigid link it was still possible to pull-up, it could generate considerable risk in real life when the rope used is flexible. Thus, further investigation needs to be performed with a more realistic rope model. The design of the RLV may also be reconsidered to include larger control surface deflections and allow more room for manoeuvrability.

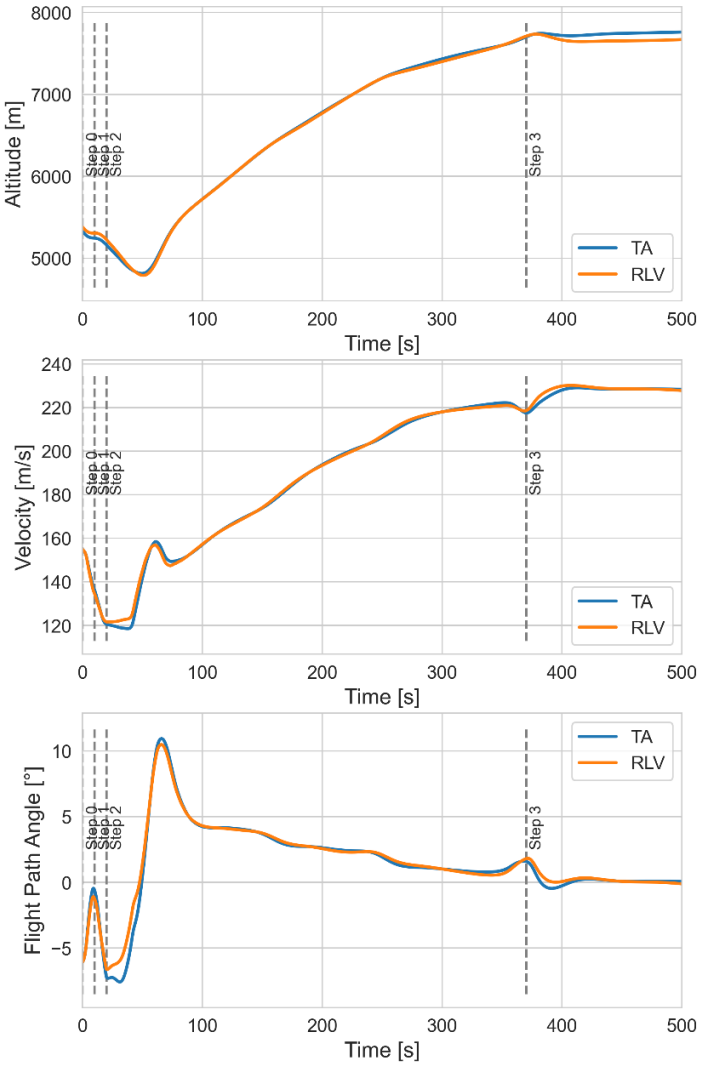

Figure 12: Pull-Up Maneouvre Trajectory without Wake

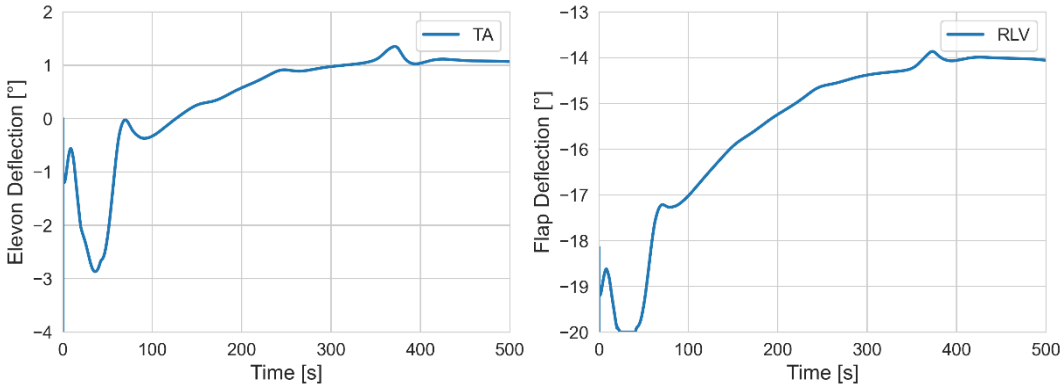

Figure 13: Control Deflection during Pull-Up Maneouvre: TA (Left) and RLV (Right)

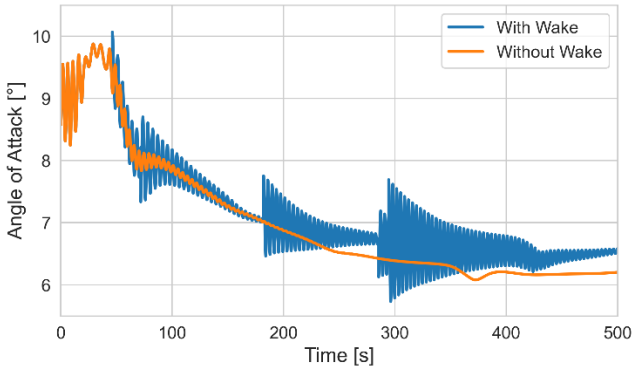

Figure 14: Sensitivity of RLV Angle of Attack to Wake during Pull-Up Maneouvre

4.2 Effect of Wake

As it was mentioned earlier in Section 2.5, the aircraft wake at higher angles of attack has a significant downwash (vertical) component that can disturb the angle of attack of the RLV when exposed to it. For an angle of attack of 12°, this component was found to reach up to 12% of free stream velocity. Such a high deficit in vertical velocity can drastically disturb the system during the pull-up and therefore, should be analysed.

Figure 14 shows the effect of wake on the RLV angle of attack. Although the RLV is not in the wake throughout the duration of the *pull-up maneouvre*, it clearly still has a considerable impact. The RLV angle of attack oscillates throughout the pull-up, which in the presence of a flexible rope can propagate and excite more oscillations leading to loss of control on the system. Additionally, it can be observed that the average angle of attack of the RLV when exposed to wake is higher than without wake. This can be attributed to the fact that the RLV sees a lower incident free stream velocity and therefore, tries to generate more lift by increasing the angle of attack. Nonetheless, future studies with a flexible rope model must analyse the effect of wake in detail.

5. Conclusion and Future Work

This study is aimed at examining the *pull-up maneouvre* phase of IAC, through simulation and analysis of full-scale test cases. For this research, the two test vehicles were chosen to be RLVC4-IIIB, which is a large winged stage weighing approximately 80 tons and the A340-600, which is a retired long-range aircraft that can support the towing loads from the large stage. During this phase, the two vehicles are assumed to be attached by a rope. The mated configuration attempts to transition from a descending flight to an ascending flight, with the end goal of reaching a suitable cruise altitude and velocity. Next, the modeling of important subsystems like aerodynamics, propulsion and external disturbances like the wake from the aircraft are discussed. The aerodynamics and wake datasets are generated through reliable CFD computations, while the performance of the airbreathing engines are modelled using GasTurb (which is an intricate tool for analysis of gas turbine performance). A simplified model of the rope modeled as a rigid link is also included in the dynamic model. The rope is assumed to be attached at the center of gravity of the TA and nose of the RLV through spherical joints that constrain translational motion but not rotational motion.

Then, using fuel consumption per range as the optimality criteria, a suitable altitude and velocity for cruise of the mated configuration is identified. Based on this, an altitude of 7800 m and a velocity of 230 m/s is given as the guidance cruise flight condition for the pull-up configuration. Independent PID controllers are proposed for both TA and RLV, to allow the vehicles to maneouvre to safety individually, in case of failure. Preliminary trajectory simulations of *pull-up maneouvre* are finally performed using these models. The mated configuration is successfully able to reach the commanded flight conditions. However, it is found that the RLV control surfaces were saturated during initial pull-up and may need some design iterations as well as further analysis. It is also found that the wake causes substantial disturbances in the RLV angle of attack. This should be analysed in detail with a flexible rope in future studies.

Acknowledgements

This work was performed under the Horizon 2020 project '**F**ormation flight for in-**A**ir **L**auncher 1st stage **C**apturing demonstrati**on**' (**FALCon**) aimed at development and testing of the "In-Air Capturing" technology. FALCon, coordinated by DLR-SART, is supported by the EU within the Programme 5.iii. Leadership in Enabling and Industrial Technologies – Space with EC grant 821953. Further information on FALCon can be found at http://www.FALCon-iac.eu

List of Abbreviations

Abbreviation	Definition
3STO	Three Stage to Orbit
CFD	Computational Fluid Dynamics
DLR	German Aerospace Center
IAC	In-Air Capturing
L/D	Lift-to-Drag
MECO	Main Engine Cut Off
PID	Proportional Integrator Derivative
RANS	Reynolds-Averaged Naviers Stokes
RLV	Reusable Launch Vehicle
TA	Towing Aircraft

Nomenclature

Symbol	Description
D	Drag force in [N]
fcr	Fuel consumption per range in [kg/m]
H	Altitude in [m]
$\dot{H}$	Rate of change of altitude in [m/s]
L	Lift force in [N]
m	Mass in [kg]
M	Mach number
sfc	Specific fuel consumption in [g/kNs]
T	Thrust in [N]
V	Velocity in [m/s]
$\dot{V}$	Acceleration in [m/s^2]
W	Weight in [N]
α	Angle of attack in [°] or [rad]
$\dot{\alpha}$	Rate of change of angle of attack in [°/s] or [rad/s]
γ	Flight path angle in [°] or [rad]
$\dot{\gamma}$	Rate of change of flight path angle in [°/s] or [rad/s]
ε	Throttle scale of the engine (between 0 to 1)

References

[1] Patentschrift (patent specification) DE 101 47 144 C1, Verfahren zum Bergen einer Stufe eines mehr-stufigen Raumtransportsystems, released 2003.

[2] M. Sippel, J. Klevanski, J. Kauffmann, "Innovative Method for Return to the Launch Site of Reusable Winged Stages," IAF-01-V.3.08, *52nd International Astronautical Congress*, 2001.

[3] S. Stappert, J. Wilken, L. Bussler, M. Sippel, "A Systematic Assessment and Comparison of Reusable First Stage Return Options", IAC-19-D2.3.10, *70th International Astronautical Congress*, 2019.
[4] M. Sippel, S. Stappert, S. Singh "RLV-Return Mode "In-Air-Capturing" and Definition of its Development Roadmap", *9th European Conference for Aeronautics and Space Sciences (EUCASS)*, 2022.
[5] S. Singh, S. Stappert, L. Bussler, M. Sippel, Y. C. Kucukosman, S. Buckingham, "A Full-Scale Simulation and Analysis of Formation Flight during In-Air Capturing", IAC-21-D2.5.2, *72nd International Astronautical Congress (IAC)*, 2021.
[6] S. Singh., S. Stappert, S. Buckingham, S. Lopes, Y.C. Kucukosman, M. Simioana, M. Pripasu, A. Wiegand, M. Sippel, P. Planquart, "Dynamic Modelling and Control of an Aerodynamically Controlled Capturing Device for 'In-Air-Capturing' of a Reusable Launch Vehicle", *11th International ESA Conference on Guidance, Navigation & Control Systems*, 2021.
[7] S. Singh, L. Bussler, S. Stappert, S. Callsen, S. Lopes, S. Buckingham, "A Superposition Approach to Aerodynamic Modelling of a Capturing Device used for In-Air Capturing of a Reusable Launch Vehicle", *9th European Conference for Aeronautics and Space Sciences (EUCASS)*, 2022.
[8] S. Singh, L. Bussler, S. Stappert, M. Sippel, S. Buckingham, S. Lopes, C. Y. Kucukosman, "Control Design and Analysis of a Capturing Device Performing In-Air Capturing of a Reusable Launch Vehicle", *9th European Conference for Aeronautics and Space Sciences (EUCASS)*, 2022.
[9] M. Sippel, S. Stappert, L. Bussler, C. Messe, "Powerful and Flexible Future Launchers in 2-or 3- stage Configuration", IAC-19-D2.4.8, *70th International Astronautical Congress (IAC)*, 2019.
[10] A340-600 Global Performer, Previous Generation Aircraft, https://www.airbus.com/aircraft/previousgeneration-aircraft/a340-family/a340-600.html, last accessed, 6 June, 2022.
[11] H. Glauert, "The Effect of Compressibility on the Lift of an Aerofoil", Proceedings of the Royal Society of London. Series A, Containing Papers of a Mathematical and Physical Character, 118(779), 113-119, 1928.
[12] European Aviation Safety Agency, EASA Type Certificate Data Sheet, Type: Rolls-Royce RB211 Trent 500 Series Engine, 2007.
[13] GasTurb GmbH: GasTurb 13, Design and Off-Design Performance of Gas Turbines, User Manual, 2018.
[14] J. Klevanski, M. Sippel, "Quasi-optimal Control for the Reentry and Return Flight of an RLV*" 5th International Conference on Launcher Technology, Missions, Control and Avionics*, S. Vol. 5, 2003.